JOURNAL OF VIROLOGY, Jan. 2005, p. 441–449 Vol. 79, No. 1
0022-538X/05/$08.00+0 doi:10.1128/JVI.79.1.441–449.2005

The Epstein-Barr Virus BILF1 Gene Encodes a G Protein-Coupled Receptor That Inhibits Phosphorylation of RNA-Dependent Protein Kinase

Patrick S. Beisser,[1]* Dennis Verzijl,[2] Yvonne K. Gruijthuijsen,[1] Erik Beuken,[1] Martine J. Smit,[2] Rob Leurs,[2] Cathrien A. Bruggeman,[1] and Cornelis Vink[1]

Department of Medical Microbiology, Cardiovascular Research Institute Maastricht, Maastricht University, Maastricht,[1] and Division of Medicinal Chemistry, Leiden/Amsterdam Center for Drug Research, Free University, Amsterdam,[2] The Netherlands

Received 7 May 2004/Accepted 12 August 2004

Epstein-Barr virus (EBV) infection is associated with many lymphoproliferative diseases, such as infectious mononucleosis and Burkitt's lymphoma. Consequently, EBV is one of the most extensively studied herpesviruses. Surprisingly, a putative G protein-coupled receptor (GPCR) gene of EBV, BILF1, has hitherto escaped attention, yet BILF1-like genes are conserved among all known lymphocryptovirus species, suggesting that they play a pivotal role in viral infection. To determine the function of EBV BILF1, the activity of this gene and its products was studied. BILF1-specific mRNA was detected in various EBV-positive cell types and found to be expressed predominantly during the immediate early and early phases of infection in vitro. Interestingly, in COS-7 cells transfected with BILF1 expression constructs, a decrease in forskolin-induced CRE-mediated transcription was measured, as well as an increase in NF-κB-mediated transcription. In contrast, CRE-mediated transcription was increased in EBV-positive Burkitt's lymphoma cells as well as EBV-positive lymphoblastoid B cells transfected with BILF1, whereas NF-κB-mediated transcription levels remained unaffected in these cells. All observed activities were sensitive to treatment with pertussis toxin, indicating that the BILF1-encoded protein mediates these activities by coupling to G proteins of the $G_{i/o}$ class. Finally, reduced levels of phosphorylated RNA-dependent antiviral protein kinase were observed in COS-7 and Burkitt's lymphoma cells transfected with BILF1. Neither of the observed effects required a ligand to interact with the BILF1 gene product, suggesting that BILF1 encodes a constitutively active GPCR capable of modulating various intracellular signaling pathways.

G protein-coupled receptors (GPCRs) belong to a superfamily of seven-transmembrane receptors that are capable of transducing signals from the outside to the cellular interior. Upon ligand binding, a large number of these receptors can alter cellular gene expression, thereby causing either differentiation, proliferation, or chemotaxis of the cell. Interestingly, some herpesviruses as well as poxviruses also encode GPCRs. Currently, four major viral GPCR gene families have been identified on the genomes of beta- and gamma-2-herpesviruses: (i) the human cytomegalovirus (HCMV) UL33 family, (ii) the HCMV UL78 family, (iii) the HCMV US28 family, and (iv) the Kaposi's sarcoma-associated herpesvirus (KSHV) ORF74 family (47). The four viral GPCR families play distinct roles in herpesvirus infection. Both the murine cytomegalovirus and rat cytomegalovirus counterparts of UL33, M33, and R33 are essential for salivary gland tropism (5, 12). The murine CMV homolog of UL78, M78, was shown to facilitate accumulation of immediate-early viral mRNA (40), and the rat CMV homolog of UL78, R78, is required for production of infectious virus in the spleen (25).

It has been postulated that US28 plays a role in chemokine scavenging (6), migration of infected smooth muscle cells (48), and cell-to-cell adhesion (21). It was shown that KSHV ORF74 can induce angiogenesis (3) and sarcomagenesis in vivo (20, 23, 38). Several of the viral GPCRs, such as those encoded by UL33, R33, US28, and KSHV ORF74, were reported to trigger intracellular signaling in a ligand-independent, constitutive fashion (1, 7, 8, 19, 46, 51), yet the viral GPCRs encoded by US28 and ORF74 can bind a variety of chemokines through which intracellular signaling is modulated (1, 14, 28). Since many mammalian GPCRs are used as targets for drug therapy, viral GPCRs are generally regarded as interesting targets for innovative antiviral drugs (47).

All interest in viral GPCRs notwithstanding, one potential viral GPCR gene, the Epstein-Barr virus (EBV) BILF1 gene (2), has hitherto escaped attention. Previously, BILF1 was recognized as a putative GPCR gene on the basis of its homology with the equine herpesvirus 2 E6 viral GPCR gene (11), yet the EBV BILF1 gene and its products have not been functionally examined. EBV, a gamma-1-herpesvirus, can establish lifelong persistence upon infection and transformation of B cells (44). EBV infection is associated with many lymphoproliferative diseases, such as infectious mononucleosis, Burkitt's lymphoma, Hodgkin's disease, and nasopharyngeal carcinoma (44). Analogous to the crucial functions of other viral GPCRs in the pathogenesis of infection, BILF1 might play an important role in EBV infection and associated diseases.

Here, we set out to determine whether the BILF1 gene encodes a biologically functional protein. We show that the

* Corresponding author. Mailing address: Department of Medical Microbiology, University Hospital Maastricht, P.O. Box 5800, 6202 AZ, Maastricht, The Netherlands. Phone: 31 43 3876642. Fax: 31 43 3876643. E-mail: pbe@lmib.azm.nl.

EBV BILF1 gene encodes a viral GPCR capable of modulating CRE-mediated signaling, stimulating NF-κB-mediated signaling and inhibiting RNA-dependent protein kinase activation.

MATERIALS AND METHODS

Cell lines and transfection. COS-7 (ATCC CRL-1651) cells were cultured and transfected as described previously (7). B95-8 (ATCC CRL 1612), HH514.c16 (22), and JY (42) cells were cultured in RPMI 1640 (Gibco, Paisley, United Kingdom) supplemented with 10% fetal bovine serum (Biochrom KG, Berlin, Germany) at 37°C and 5% CO_2 in an incubator.

Expression constructs. DNA was extracted from B95-8 cells with an Xtrax DNA isolation kit (Gull Laboratories, Salt lake City, Utah) and subjected to PCR. The following primers were used to amplify the predicted BILF1 open reading frame (ORF): primer 1, AATTGGTACC*TCTGACCAGCAAGATGCT CTCCACCAT*; primer 2, AATTGGTACC*ATGGCCCCCGGGTCCACC*; and primer 3, TATTGGATCC*TCAGGTGGACTGGCTAGGCACCC*. The sequences in italics are derived from GenBank accession number NC_001345. With primers 1 and 3, a fragment which contained the complete BILF1 ORF was generated, termed BILF1A. The PCR that included primers 2 and 3 resulted in a fragment containing a shorter variant of the BILF1 ORF which starts 10 bp downstream of the first ATG and was termed BILF1B. The PCR products were digested with Asp718I and BamHI and ligated into Asp718I- and BamHI-digested expression vector pcDEF3 (18), resulting in constructs pBILF1A and pBILF1B.

Two additional expression constructs were used as positive controls. The first contains human CMV (HCMV) UL33 and was made as follows. Plasmid p472 (pcDNA3 containing the HCMV UL33 ORF) (8) was digested with HindIII, treated with Klenow DNA polymerase, and subsequently digested with NotI. Then, the insert was ligated in EcoRV- and NotI-digested pcDEF3, resulting in plasmid pUL33. The second control plasmid contains KSHV ORF74, designated pORF74 (46). The CRE reporter plasmid pTLNC-21CRE was obtained from W. Born (National Jewish Medical and Research Center, Denver, Colo.) (13). The NF-κB reporter plasmid pNF-κB-Luc is from Stratagene (BD Biosciences, Alphen aan de Rijn, The Netherlands).

Quantitative RT-PCR. Total RNA isolates from EBV-positive cell lines B95-8, JY, HH514.c16, C666-1, Namalwa, and X50 as well as from the EBV-negative cell line Ramos were generously provided by Servi Stevens (Department of Pathology, Free University of Amsterdam, Amsterdam, The Netherlands). Each of the RNA samples used for cDNA synthesis was derived from 5×10^5 cells. The RNA samples were treated with DNase in a mixture containing 40 mM Tris-HCl pH 7.4, 6 mM $MgCl_2$, 2 mM dithiothreitol, 7 U of RNA Guard (Amersham Pharmacia Biotech, Roosendaal, The Netherlands), and 2.5 U of DNase I (Amersham Pharmacia Biotech) in a final reaction volume of 50 μl. After 1.5 h, the RNA samples were precipitated with isopropanol. The pellets were washed with 70% ethanol and dissolved in H_2O.

Half of each RNA sample was included in a reverse transcription (RT) reaction, which contained 2.5 μM random hexanucleotide mixture (Applied Biosystems, Nieuwerkerk aan de IJssel, The Netherlands), first-strand buffer (Invitrogen Life Technologies, Breda, The Netherlands), 10 μM dithiothreitol, 200 μM deoxynucleoside triphosphates, 7 U of RNA Guard (APB), and 50 U of SuperScript II (Invitrogen Life Technologies), in a final volume of 20 μl. The other half of each RNA sample was included in reaction mixtures from which reverse transcriptase was omitted. All mixtures were incubated at 42°C for 1 h, followed by a reverse transcriptase inactivation step at 70°C for 10 min. Finally, they were diluted by adding Tris-EDTA to a final volume of 100 μl; 5-μl samples (corresponding to 2.5×10^4 cells) were added to PCR mixtures with a total volume of 50 μl, containing PCR buffer (Qiagen, Leusden, The Netherlands), 200 μM deoxynucleoside triphosphates, 1.25 U of HotStarTaq (Qiagen),, and 400 nM primer 4, GGTATGGCGTTGGAGAAGA, and primer 5, TAATCAGCAGGA GTACCAGACAAA (derived from GenBank accession no. NC_001345).

PCR was performed on a GeneAmp PCR Systems 9600 thermal cycler (Perkin Elmer, Nieuwerkerk aan de IJssel, The Netherlands) for 4 min at 95°C, followed by 40 cycles of 1 min at 95°C, 1 min at 55°C, and 1 min at 72°C, and finally 7 min at 72°C. Samples were analyzed by agarose gel electrophoresis and subsequent staining with ethidium bromide. For quantitative PCR, 5-μl cDNA samples (corresponding to 2.5×10^4 cells) were added to 50-μl reaction mixtures, each containing Taqman Universal PCR Master Mix (Applied Biosystems), 900 nM each of primers 4 and 5, and 125 nM TaqMan probe, 5-carboxyfluorescein-AA CCTCCCACAGAAATGTGTGCCTGTAC-5-carboxytetramethylrhodamine (GenBank accession no. NC_001345). The reactions were performed in 96-well microtiter plates under the following conditions: 2 min at 50°C and 10 min at 95°C, followed by 42 cycles of 95°C for 15 s and 60°C for 1 min. Data were analyzed with the ABI Prism 7000 sequence detection system software (Applied Biosystems). For quantification of cDNA molecules, standard curves were gener ated with dilutions of quantified plasmid pBILF1A.

Reporter gene and inositol phosphate assays. Reporter assays for CRE and NF-κB signaling in COS-7 cells were performed as described previously (19). In the CRE assay, COS-7 cells were transfected with 5 μg of the reporter plasmid pTLNC-21CRE (containing a luciferase gene controlled by a CRE-specific promoter) (13) and 5 μg of either pcDEF3, pBILF1A, or pBILF1. In the NF-κB assay, cells were transfected with 5 μg of the reporter plasmid pNF-κB-Luc (containing a luciferase gene controlled by an NF-κB-specific promoter) (BD Biosciences, Alphen aan de Rijn, The Netherlands) and 2 μg of either pcDEF3, pBILF1A, or pBILF1B. Dulbecco's modified Eagle's medium without serum and either with or without pertussis toxin (100 ng/ml) was added to the cells immediately after transfection. COS-7 cells containing pTLNC-21CRE were treated with 10 μM forskolin at 18 h after transfection. At 24 h after transfection, these cells were lysed and luciferase activities were measured. Luciferase activities in lysates from COS-7 cells containing pNF-κB-Luc were measured at 48 h after transfection.

The reporter assays were adapted for HH514.c16 and JY cells as follows: 10^7 cells were suspended in 400 μl of 27 mM sodium phosphate (pH 7.5) and 150 mM sucrose and mixed with 5 μg of reporter plasmid pTLNC-21CRE or pNF-κB-Luc and 2 to 5 μg of either pcDEF3, pBILF1A, or pBILF1B. The suspensions were transferred to 0.4-cm electroporation cuvettes (Bio-Rad Laboratories, Veenendaal, The Netherlands), incubated on ice for 10 min, and electroporated with a Gene Pulser II apparatus equipped with a radio frequency (RF) module (Bio-Rad Laboratories). The RF module was set to 340 V, 40 kHz, 100% modulation, 4 ms per burst, five bursts, and a 1-s burst interval. After electroporation, the cuvettes were incubated on ice for 10 min, and the contents were transferred to 12-well plates containing RPMI medium without serum with or without 100 ng of pertussis toxin per ml and kept at 37°C in a 5% CO_2 incubator. At 24 to 48 h after transfection, suspensions were pelleted and lysed, and luciferase activities were measured. Myo-[^{3}H]inositol phosphate accumulation in transfected COS-7 cells was determined as described previously (7). In each of the experiments, samples were analyzed in triplicate. Experiments were performed at least three times.

SDS-PAGE and Western blotting. Pellets of COS-7 and HH514.c16 cells, each consisting of 10^7 cells, were lysed in a solution containing 20 mM morpholinepropanesulfonic acid (MOPS, pH 7.0), 2 mM EGTA, 5 mM EDTA, 30 mM sodium fluoride, 40 mM β-glycerophosphate, 10 mM sodium pyrophosphate, 2 mM sodium orthovanadate, and 0.5% (wt/vol) Nonidet P-40 at 0°C. The lysed samples were centrifuged for 1 h at $24{,}000 \times g$. Supernatant fractions containing 100 μg of protein were mixed with sodium dodecyl sulfate (SDS)-polyacrylamide gel electrophoresis (PAGE) sample buffer, boiled for 5 min, and separated by SDS–12% PAGE, according to the Laemmli method (31). The separated proteins were transferred to a Hybond C-Super membrane (Amersham Pharmacia Biotech) and incubated with either anti-RNA-dependent protein kinase (PKR) (Upstate Biotechnology/Brunswig Chemie, Amsterdam, The Netherlands) or anti-phospho-T^{451}-PKR (BioSource International, Nivelles, Belgium) polyclonal antibodies, followed by incubation with peroxidase-conjugated goat anti-rabbit monoclonal antibodies (Dako, Glostrup, Denmark).

The protein bands were detected with the ECL luminescence detection system (Amersham Pharmacia Biotech) and recorded with the FluorChem image analysis system (Alpha Innotech Corporation, San Leandro, Calif.). Band intensities were quantified with image analysis program ImageJ (version 1.31; Research Services Branch, National Institute of Mental Health, Bethesda, Md. [http://rsb.info.nih.gov/ij]). All experiments were performed at least three times.

RESULTS

EBV BILF1 is member of a distinct GPCR-like gene family. Both the sequences and genomic positions of BILF1-like genes are conserved among all of the currently known gamma-1-herpesviruses. In addition, BILF1 homologs are found in a subset of gamma-2-herpesvirus species. As shown in Fig. 1, each member of the BILF1 family is positioned at the 5′ end of a conserved gene block that includes the viral DNA polymerase gene. The ORF74-like genes, however, are positioned near another conserved gene block that includes the large tegument

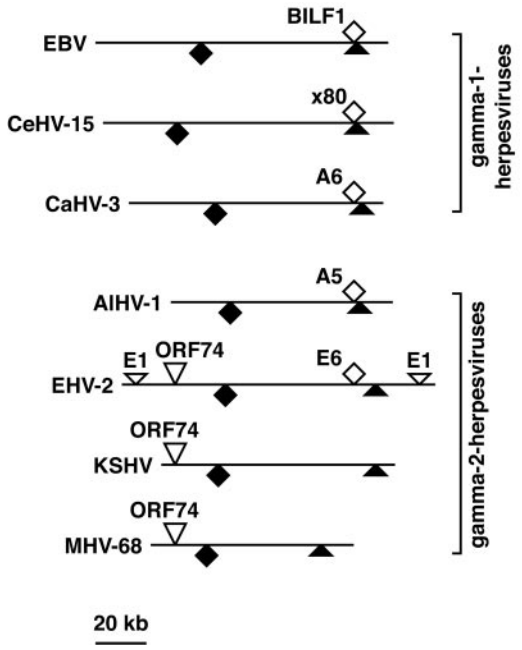

FIG. 1. EBV BILF1 and KSHV ORF74 belong to different viral GPCR gene families. The lines represent herpesvirus genomes. The symbols indicate gene positions, which were derived from GenBank accession nos. AY037858, NC_001345, NC_001650, NC_001826, NC_002531, NC_003409, and NC_004367. Open symbols represent viral GPCR genes. The names of viral GPCR genes are indicated above their corresponding symbols. Genomes and gene positions are drawn to scale. EBV, Epstein-Barr virus; CeHV15, cercopithecine herpesvirus 15; CaHV-3, callitrichine herpesvirus 3; AlHV-1, alcephaline herpesvirus 1; EHV2, equine herpesvirus 2; KSHV, Kaposi's sarcoma-associated herpesvirus; MHV-68, murine gammaherpesvirus 68; ◇, BILF1 family; ▽, ORF74 family; ⌓, equine herpesvirus 2 E1; ♦, large tegument protein family; ▲, DNA polymerase family.

protein gene. This indicates that BILF1 represents an independent, as yet uncharacterized, family of herpesvirus GPCR genes.

BILF1 is transcribed in various EBV-positive cell lines. To examine the kinetics of BILF1 expression during EBV infection, RNA samples derived from several EBV-positive cell types were subjected to RT-PCR analysis. First, RNA samples were prepared from the Burkitt's lymphoma cell line HH514.c16, in which EBV gene expression is highly restricted to latency type I (22, 35). The samples were taken from untreated cells as well as from cells in which EBV replication was stimulated by phorbol ester and butyrate treatment (49). In addition, these treatments were also carried out in the presence of phosphonoacetic acid in order to block viral DNA replication and EBV late-phase protein expression. The RNA samples were subjected to BILF1-specific RT-PCR in either the presence or absence of reverse transcriptase. BILF1-specific fragments were detected in all reverse transcriptase-treated samples but not in untreated samples (Fig. 2A), indicating that BILF1-specific cDNA rather than viral genomic DNA was detected.

BILF1 mRNA levels were quantified by real-time PCR. Approximately 10^4 BILF1-specific RNA copies per 10^6 HH514.c16 cells were measured in samples derived from unstimulated cells (Fig. 2B). At 1, 2, 4, and 5 days after EBV stimulation, RNA levels were approximately 100 times higher than before stimulation (Fig. 2B). These levels were similar in both phosphonoacetic acid-treated and untreated cells. The results indicate that BILF1 transcription is correlated with activation of EBV replication, yet transcription occurs independently of viral DNA replication, suggesting that BILF1 is either an immediate-early or early gene.

To measure BILF1 transcription levels in other cell types, RNA samples from the following lines were included in a subsequent RT-PCR assay: B95-8 (an EBV-positive marmoset lymphoblastoid cell line) (36), JY (lymphoblastoid cell line derived from human lymphocytes infected with B95-8-derived EBV) (42), X50-7 (lymphoblastoid cell line derived from human umbilical cord lymphocytes infected with EBV B98-8) (37), C666-1 (a nasopharyngeal carcinoma cell line) (24), Namalwa (an EBV-positive Burkitt's lymphoma cell line) (32), and Ramos (an EBV-negative Burkitt's lymphoma cell line) (29). PCR fragments were generated with all reverse transcriptase-treated samples with the exception of those derived from Ramos cells (Fig. 2C).

In order to quantify BILF1 mRNA levels, the cDNA samples from each of the cell lines were analyzed by real-time PCR. As shown in Fig. 2D, BILF1 mRNA levels ranged between approximately 10^3 and 10^5 copies per 10^6 cells. This indicated that the level of BILF1 transcription in various of EBV-positive cell lines is 10 to 100 times lower than that in stimulated HH514.c16 cells (Fig. 2B). The low level of BILF1 mRNA expression in Namalwa cells is comparable to the level observed in uninduced HH514.c16 cells and correlates with the restricted EBV latency I type in both cell lines. The intermediate levels of BILF1 expression in noninduced B-cell lines B95-8, JY, and X50/7 and the nasopharyngeal carcinoma line C666-1 may be related to the spontaneous lytic cycle induction in 1 to 5% of the cells of each of these lines (24, 41). We conclude that BILF1 is transcribed (i) at low levels in unstimulated EBV-positive B-cell lines under tight latency, (ii) at intermediate levels in lymphoblastoid cell line and the nasopharyngeal carcinoma-derived C666-1 line, and (iii) at high levels upon full induction of the lytic cycle.

EBV GPCR signals through $G_{i/o}$ but not through $G_{q/11}$. To determine whether EBV BILF1 encodes a functional GPCR, we set out to generate BILF1 expression constructs. Previously, the ATG initiation codon of the BILF-1 open reading frame was predicted to be localized to positions 151703 to 151701 of the EBV sequence (GenBank accession no. NC_001345). However, 10 bp downstream of this codon, a second ATG is present. In contrast to the "first" ATG, the second conforms to the Kozak consensus for eukaryotic translation initiation sites (30), which would favor the second ATG as the authentic initiation codon. However, we found the first eight amino acid residues of BILF1 to be identical to those of its homolog from cercopithecine herpesvirus 15, with the exception of the second methionine, which is a leucine in the cercopithecine herpesvirus BILF1-like sequence. This observation would predict the first ATG as the authentic initiation codon. Based on these considerations, two different expression plasmids were made, one containing the BILF1 ORF beginning at the first putative start codon (plasmid pBILF1A) and

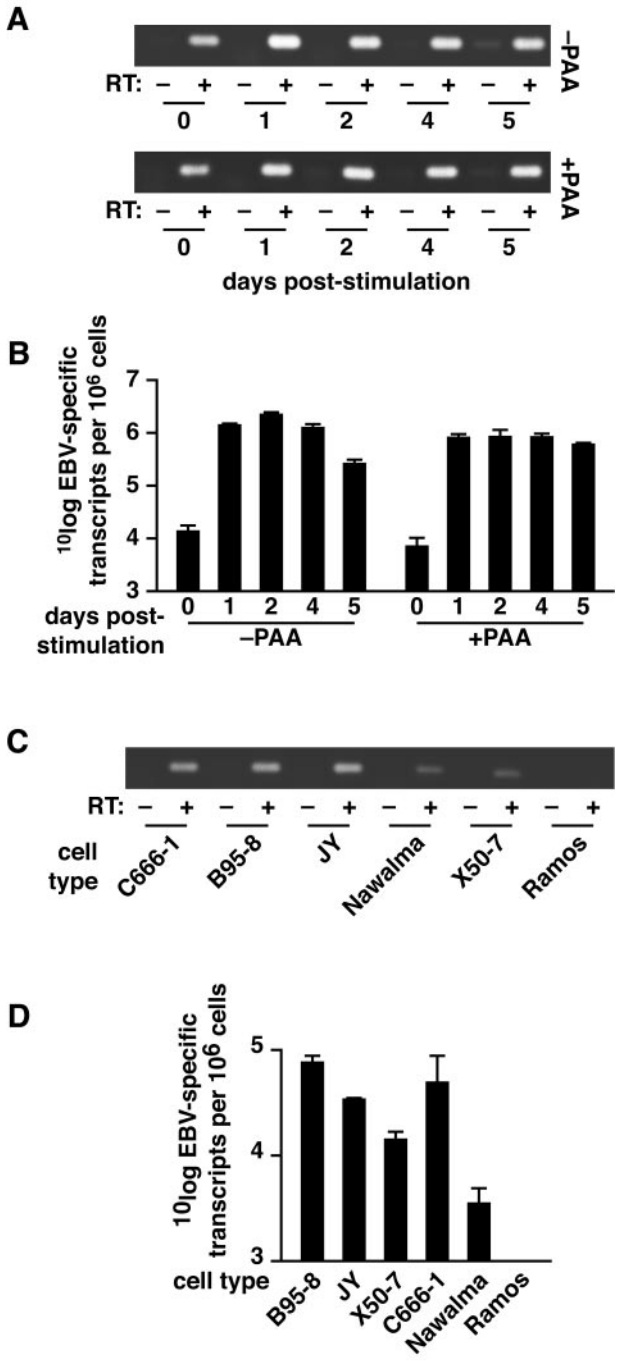

FIG. 2. EBV BILF1 is an early-phase gene that is transcribed in various EBV-positive cell types. (A) The BILF1-specific RT-PCR assay detects cDNA but not genomic EBV DNA in HHV514.c16 cells. Each panel represents an ethidium bromide-stained agarose gel containing RT-PCR fragments. (B) BILF1 transcription is upregulated in HH514.16c cells stimulated with phorbol ester and butyric acid and either with or without phosphonoacetic acid treatment. The graph indicates BILF1-specific RNA levels measured by TaqMan reactions. (C) The BILF1-specific RT-PCR assay detects cDNA but not genomic EBV DNA in various EBV-positive cell types. (D) BILF1-specific RNA levels in various EBV-positive cell lines. The effectiveness of the phosphonoacetic acid treatment was confirmed by immunoblot, in which the late-phase EBV viral capsid antigen could not be detected (data not shown). RT, reverse transcriptase; PAA, phosphonoacetic acid; C666-1, a nasopharyngeal carcinoma cell line; B95-8, an EBV-positive marmoset lymphoblastoid cell line; JY, an EBV-positive human lymphoblastoid cell line; Namalwa, an EBV-positive Burkitt's lymphoma cell line; X50, a cord blood-derived EBV-positive lymphoblastoid cell line; Ramos, an EBV-negative Burkitt's lymphoma cell line.

the other containing the BILF1 ORF beginning at the second putative start codon (plasmid pBILF1B).

To assess whether the EBV GPCR possesses signaling activity, two types of assays were performed, each of which involved a reporter gene, luciferase, under the control of a promoter containing either CRE-specific or NF-κB-specific elements. In the first reporter gene experiment with COS-7 cells, a CRE reporter plasmid was cotransfected with either plasmid pBILF1A, pBILF1B, pcDEF3 as a negative control, or pORF74 as a positive control. As a result, a slight decrease in CRE-driven gene activation was observed in cells transfected with pBILF1A, pBILF1B, or pORF74 (data not shown). Since CRE-driven gene activation induced by forskolin can be inhibited through $G_{i/o}$-mediated signaling, cells were incubated with forskolin in either the presence or absence of the $G_{i/o}$ inhibitor pertussis toxin. Interestingly, the luciferase activities in cells transfected with either pBILF1A, pBILF1B or pORF74 were significantly lower (65 to 86%) than those in cells transfected with pcDEF3 (Fig. 3A), indicating that expression of BILF1 inhibits forskolin-induced CRE-driven gene activation. Moreover, pertussis toxin treatment of cells transfected with pBILF1A or pBILF1B reversed the inhibition of CRE-driven gene activation (Fig. 3A), indicating that BILF1 expression inhibits CRE-driven gene activation through $G_{i/o}$ coupling. When increasing concentrations of either pBILF1A or pBILF1B were used for transfection, decreasing levels of luciferase activity were found (Fig. 3B). Thus, BILF1/$G_{i/o}$-mediated signaling is BILF1 expression level dependent. Taken together, these results show that the EBV BILF1 gene encodes a functional $G_{i/o}$-coupling GPCR. Since the signaling assays were performed in serum-free medium, it is likely that the EBV GPCR signals in a ligand-independent, constitutive fashion.

To study EBV GPCR signaling in cells types relevant to EBV infection, the CRE reporter gene assay was performed with the EBV-positive Burkitt's lymphoma line HH514.c16. Surprisingly, luciferase activities in HH514.c16 cells transfected with either pBILF1A or pBILF1B were 170 to 200% of that in cells transfected with the negative control DNA pcDEF3 (Fig. 3C). Upon pertussis toxin treatment (Fig. 3C), this activity was reduced to negative-control levels, indicating that viral GPCR signals in a $G_{i/o}$-dependent manner. Similar results were obtained by repeating this experiment with an EBV-positive lymphoblastoid B-cell line, JY. CRE activity in JY cells transfected with either BILF1A or BILF1B was increased to 280 to 300% of that in cells transfected with the negative control DNA pcDEF3 (Fig. 3D). Similar to HH514.c16 cells, this activity could be reduced to negative-control levels by pertussis toxin treatment (Fig. 3D).

To determine whether the difference in BILF1-mediated responses between COS-7 and B cells was specific for BILF1 or represented a more general phenomenon, the CRE assay was repeated with the KSHV ORF74 gene. Similar to BILF1A and

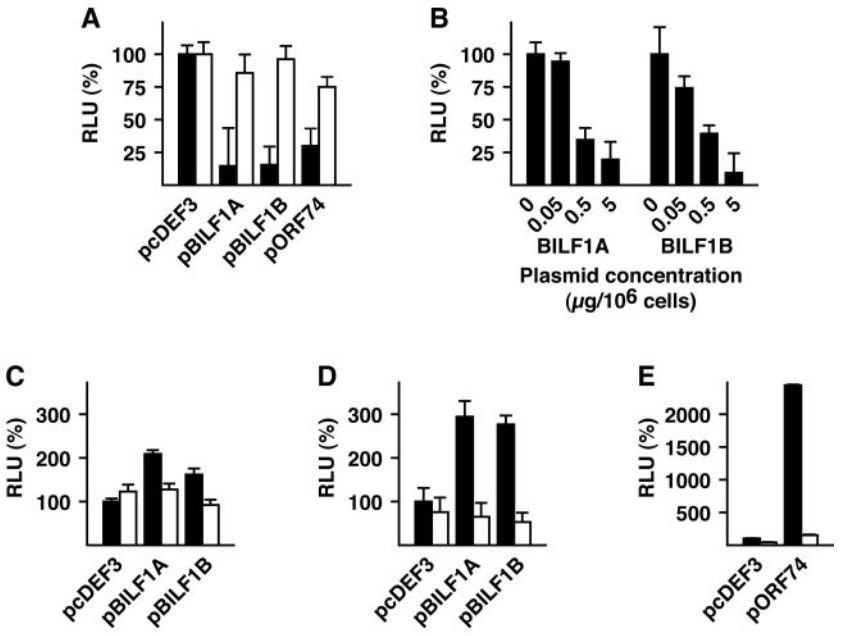

FIG. 3. BILF1 drives CRE-mediated gene expression. CRE-driven luciferase expression in COS-7 cells transiently cotransfected with reporter plasmid pTLNC-21CRE and 5 μg (A) or increasing amounts (B) of either pcDEF3, pcDEF3/BILF1A, or pcDEF3/BILF1B. Cells were stimulated with forskolin (10 μM) for 6 h before luciferase activities were measured. When amounts of either pcDEF3/BILF1A or pcDEF3/BILF1B lower than 5 μg were used, pcDEF3 was added to a total of 5 μg of plasmid DNA per transfection. CRE-driven luciferase expression in HH514.c16 (C) and JY (D) cells transiently transfected with reporter plasmid pTLNC-21CRE and either pcDEF3, pcDEF3/BILF1A, or pcDEF3/BILF1B. (E) CRE-driven luciferase expression in JY cells transiently transfected with pTLNC-21CRE and either pcDEF3 or pORF74. RLU, relative light units, expressed as a percentage of the value obtained with pcDEF3.

BILF1B, ORF74 expression significantly reduces CRE-mediated gene activation in COS-7 cells (Fig. 3A), whereas pORF74 expression increases CRE-mediated gene activation in HH514.c16 cells (data not shown) and JY cells (Fig. 3E). We therefore hypothesize that the differential CRE response in COS-7 and B cells is cell type rather than receptor dependent.

In a second reporter gene experiment, an NF-κB reporter plasmid was cotransfected with either pcDEF3, pBILF1A, or pBILF1B in COS-7 cells. NF-κB-mediated transcription in cells transfected with either pBILF1A or pBILF1B was significantly higher (up to 300% of the negative-control levels) than in cells transfected with pcDEF3 (Fig. 4A). In contrast, luciferase activities in lysates from pertussis toxin-treated cells transfected with pBILF1A or pBILF1B did not differ significantly from those derived from cells transfected with pcDEF3 (Fig. 4A). This shows that, like the CRE-driven transcription, the NF-κB-driven gene activation by BILF1 in COS-7 cells is also mediated by coupling to $G_{i/o}$ proteins. As shown in Fig. 4B, transfection of increasing concentrations of either pBILF1A or pBILF1B resulted in increasing levels of luciferase activity. This indicates that BILF1-mediated NF-κB activation is expression level dependent.

To determine whether the EBV GPCR also signals to NF-κB in physiologically relevant cell types, the NF-κB reporter gene assay was repeated with cell lines HH514.c16 and JY. However, in contrast to the activity of viral GPCR in COS-7 cells, the receptor did not induce detectable levels of NF-κB-driven transcription in either HH514.c16 or JY cells (Fig. 4C and D). The differences in BILF1-mediated signaling between COS-7 cells and both HH514.c16 and JY cells are most likely due to differential expression of downstream signaling partners within these cell lines, such as increased levels of endogenous NF-κB in EBV-infected cells (27).

In addition to the assessment of EBV GPCR coupling to $G_{i/0}$ by conducting reporter gene assays, the possibility of EBV GPCR coupling to another G protein class was examined. COS-7 cells endogenously express two members of the G_q class, G_q and G_{11} (53). Upon activation, $G_{q/11}$ proteins trigger phospholipase Cβ-mediated signaling, which was assessed by measuring the accumulation of inositol phosphate. Cells transfected with either pcDEF3, pBILF1A, pBILF1B, pUL33, or pORF74 were incubated with ^{3}H-labeled inositol, after which accumulation of radiolabeled inositol phosphate was measured. Cells transfected with either pUL33 or pORF74 contained significantly higher levels of radiolabeled inositol phosphate than cells transfected with pcDEF3 (Fig. 5). By contrast, radiolabeled inositol phosphate levels in cells transfected with either pBILF1A or pBILF1B were similar to those in pcDEF3-transfected cells (Fig. 5), indicating that the BILF1 gene product does not constitutively signal through the phospholipase Cβ pathway via $G_{q/11}$.

EBV GPCR induces inhibition of PKR phosphorylation. To examine the influence of the EBV GPCR on the phosphorylation status of cellular protein kinases, extracts of viral GPCR-expressing COS-7 cells were used in an immunoblot screen with an array of antibodies directed against a variety of phosphoproteins (Kinetworks Phospho-site screen 1.3; Kinexus, Vancouver, Canada). Interestingly, this screen revealed a significant change in the level of phosphorylated RNA-dependent protein kinase (PKR) upon BILF1 expression (data not

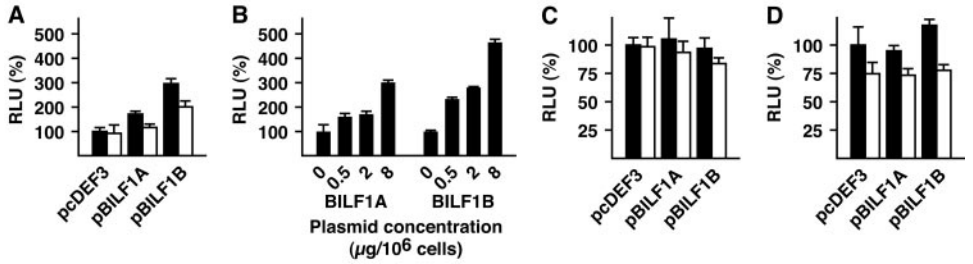

FIG. 4. BILF1 drives NF-κB-mediated gene expression. NF-κB-driven luciferase expression in COS-7 cells transiently transfected with reporter plasmid pNF-κB-Luc and 2 μg (A) or increasing amounts (B) of either pcDEF3, pcDEF3/BILF1A, or pcDEF3/BILF1B. When amounts of either pcDEF3/BILF1A or pcDEF3/BILF1B lower than 8 μg were used, pcDEF3 was added to a total of 8 μg of plasmid DNA per transfection. NF-κB-driven luciferase expression in HH514.c16 (C) and JY (D) cells transiently transfected with reporter plasmid pNF-κB-Luc and either pcDEF3, pcDEF3/BILF1A, or pcDEF3/BILF1B. RLU, relative light units, expressed as a percentage of the value obtained with pcDEF3. Solid bars, untreated; open bars, pertussis toxin treated (100 ng/ml).

shown). PKR is an interferon-inducible enzyme that plays an important role in intracellular antiviral defense (26). Phosphorylation of PKR can result in shutdown of cellular protein synthesis and apoptosis (52). The viral GPCR-induced change in the phosphorylation status of PKR was investigated further by subjecting extracts of COS-7 cells transfected with either pcDEF3, pBILF1A, or pBILF1B to immunoblot analysis with antibodies specific for either PKR or phospho-PKR. The anti-PKR antibodies were used to normalize the total cellular PKR levels between the different samples and as a reference for phospho-PKR levels. The anti-phospho-PKR antibodies were used to measure PKR phosphorylation levels at residue T^{451}, a residue essential for PKR activation (34).

As shown in Fig. 6A, the levels of PKR did not differ significantly between pcDEF3-, pBILF1A-, and pBILF1B-transfected cells (lanes 1, 2, and 3, respectively). By contrast, the levels of phosphorylated PKR in cells transfected with either pBILF1A or pBILF1B (Fig. 6A, lanes 5 and 6, respectively) are significantly lower, 20% and 40%, respectively, relative to the negative control level in pcDEF3-transfected cells (Fig. 6A, lane 4). Similar effects were observed in HH514.c16 cells. Whereas total cellular PKR levels were similar in all samples (Fig. 6B, lanes 1 to 6), the levels of phospho-PKR in cells transfected with either pBILF1A or pBILF1B (Fig. 6B, lanes 9 and 11) were 39% and 21%, respectively, relative to the basal level in pcDEF3-transfected cells (Fig. 6B, lane 7). Interestingly, phospho-PKR levels were also lower, 24% and 16% in pBILF1A- and pBILF1B-transfected HH514.c16 cells treated with pertussis toxin, respectively (Fig. 6B, lanes 10 and 12). Thus, the BILF1-mediated decrease in PKR phosphorylation at residue T^{451} is independent of $G_{i/o}$ coupling.

In summary, while total PKR levels remain constant, the phosphorylation of PKR at T^{451} is downregulated upon EBV GPCR expression. By virtue of this activity, the EBV GPCR inhibits a crucial cellular antiviral response pathway. Although inhibition of this pathway has previously been described for several other viral proteins, EBV GPCR represents the first example of a GPCR that inhibits PKR phosphorylation.

DISCUSSION

This is the first report of a functional GPCR encoded by a gamma-1-herpesvirus gene, EBV BILF1. Until now, genes coding for such viral GPCRs had been identified exclusively on the genomes of poxviruses and beta- and gamma-2-herpesviruses (reviewed in references 39 and 47). The BILF1 gene was identified following the sequencing of the complete EBV genome (2). The gene was subsequently predicted to encode a seven-transmembrane protein (4) and reported to show sequence similarity with the putative equine herpesvirus 2 viral GPCR gene E6 (11). In this study, we have demonstrated that BILF1 encodes a functional GPCR which is able to couple to proteins of the $G_{i/o}$ class. This coupling results in differential effects on CRE-mediated gene expression in different cell lines: a decrease in CRE-driven expression is seen in COS-7 cells, whereas an increase is seen in HH514.c16 and JY cells. This difference is not unique for the BILF1-encoded viral GPCR, as KSHV ORF74 differentially modulates CRE-mediated gene expression in these cell types in a similar fashion. We hypothesize that these differential effects are caused by the expression and, thus, activation of different subsets of G proteins in COS-7 cells on the one hand and B-cell lines on the other.

Another consequence of the activation of $G_{i/o}$ proteins by the BILF1-encoded GPCR in COS-7 cells is upregulation of NF-κB-mediated gene expression. In addition, we found that BILF1 expression resulted in inhibition of RNA-dependent protein kinase activation, independent of coupling to $G_{i/o}$ proteins. This suggests the coupling of the BILF1 gene product to

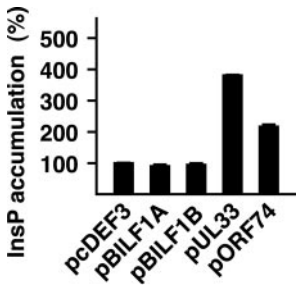

FIG. 5. Viral GPCR-mediated induction of inositol phosphate (InsP) accumulation. COS-7 cells were transiently transfected with either pcDEF3, pcDEF3/BILF1A, pcDEF3/BILF1B, pcDEF3/UL33, or pcDEF3/ORF74. At 48 h after transfection, inositol phosphate accumulation was measured and is expressed as a percentage of that in pcDEF3.

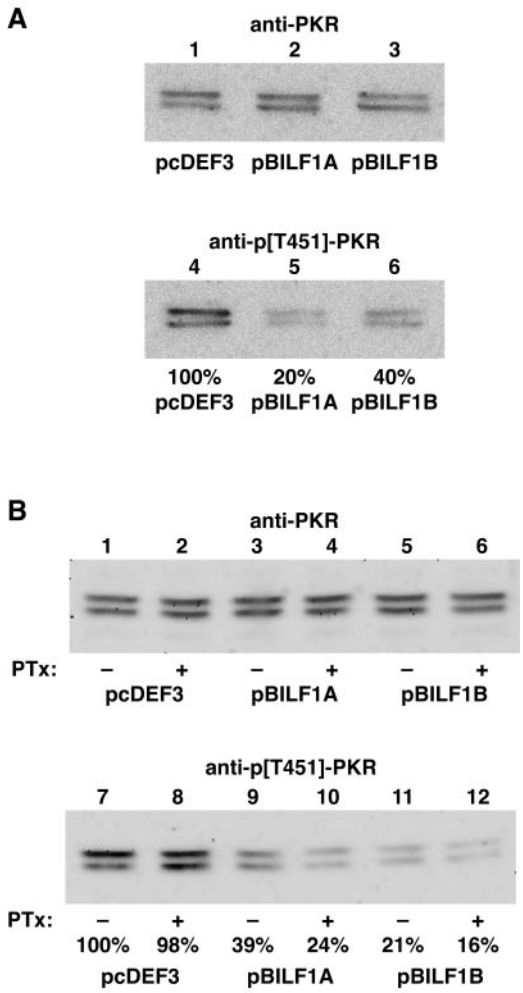

FIG. 6. BILF1 expression inhibits PKR phosphorylation. Cytoplasmic lysates of cells transfected with either pcDEF3, pcDEF3/BILF1A, or pcDEF3/BILF1B were separated by SDS–12% PAGE and transferred to a carrier membrane. The blots were stained with monoclonal antibodies specific for either PKR or phospho-T^{451}-PKR and visualized by chemiluminescence. (A) Chemiluminogram of a Western blot containing COS-7 cell lysates and (B) HH514.c16 cell lysates. PTx, pertussis toxin.

other G protein signaling pathways. Moreover, each of these responses occurred in the absence of any exogenously added ligands, suggesting that EBV GPCR possesses ligand-independent, constitutive signaling activity. Previously, members of three other viral GPCR families were found to display constitutive activity through coupling to different G proteins. The HCMV UL33-encoded viral GPCR is active through G_s, $G_{i/o}$, and G_q coupling (8). The HCMV US28-encoded GCPR is constitutively active through association with $G_{q/11}$ (7). The viral GPCR encoded by KSHV ORF74 is constitutively active through $G_{i/o}$ (10, 46) and $G_{q/11}$ coupling (1) and $G_{\alpha 13}$ (45). In contrast to the KSHV GPCR, we found that EBV GPCR was unable to mediate constitutive inositol phosphate-related signaling through $G_{q/11}$ coupling. This shows that these receptors have fundamentally different properties. Whether the EBV GPCR is able to interact constitutively with alternative G protein classes, such as $G_{12/13}$, remains to be investigated.

Of all GPCRs other than those encoded by members of the BILF1 gene family, human CXCR3A and KSHV GPCR show the highest homology with EBV GPCR (20.8% and 21.2%, respectively). The human chemokine receptor CXCR3A can interact with the CXC chemokines CXCL9/MIG, CXCL10/IP-10, and CXCL11/IP-9 (9, 33). The KSHV-encoded viral GPCR can interact with CXC chemokines CXCL1/GROα, CXCL8/IL-8, and CXCL10/IP-10 as well as KSHV vMIP-II (1, 15, 16, 17). Several experiments were performed to determine whether EBV GPCR interacts with these chemokines as well as with chemokines of the CC and CX3C families. However, in an assay with radiolabeled CXCL1/GROα, CXCL8/IL-8, CXCL10/IP-10, CCL4/MIP-1β, CCL5/RANTES, and CX3CL1/fractalkine, none of these chemokines were able to bind specifically to BILF1-expressing cells (data not shown). Additionally, several chemokine species, CCL2/MCP-1, CCL3/MIP-1α, CCL4/MIP-1β, CCL5/RANTES, CCL11/eotaxin, CCL19/MIP-3β, CXCL1/GROα, CXCL4/PF-4, CXCL8/IL-8, CXCL9/MIG, CXCL10/IP-10, CXCL11/IP-9, CXCL12a/SDF-1α, CX3CL1/fractalkine, and KSHV vMIP-II, were assayed for their ability to alter intracellular signaling in BILF1-transfected cells, but none of these chemokines was found to have a significant effect on InsP accumulation or either cyclic AMP- or NF-κB-mediated signaling (data not shown). Consequently, the EBV GPCR remains an orphan receptor. Nevertheless, the search for chemokines and other ligands which could potentially bind to this receptor is still in progress.

Expression of EBV GPCR results in reduction of cellular PKR phosphorylation. PKR is a double-stranded RNA-dependent protein kinase that functions in cellular antiviral defense by shutting down the host protein synthesis system and inducing apoptosis (26). Our data suggest that the EBV GPCR can interfere with this cellular antiviral defense system. Moreover, EBV GPCR is the first GPCR reported to be capable of altering PKR phosphorylation levels. Previously, we determined that the rat cytomegalovirus R33 gene, which encodes a constitutively active GPCR, did not affect PKR phosphorylation in transfected COS-7 cells (data not shown). This indicates that PKR inhibition is not a general phenomenon induced upon viral GPCR expression. Until now, alteration of PKR phosphorylation was only reported for cellular non-GPCR-related signal transduction pathways, such as those triggered by viral double-stranded RNA, lipopolysaccharide, interleukin-1, tumor necrosis factor alpha, heat shock, platelet-derived growth factor, or interleukin-3 deprivation (reviewed in reference 52). Some EBV-specific factors, such as the RNA molecules EBER1 and EBER3 (50), as well as the lytic-phase post-translational regulator protein SM (43) were also shown to reduce PKR phosphorylation. Thus, the discovery of EBV GPCR-dependent PKR inhibition sheds new light on the PKR-mediated cellular response to biological stress. Future studies will focus on elucidation of the signaling pathways through which BILF1 mediates inhibition of PKR phosphorylation.

It was previously reported that BILF1-derived transcripts are expressed in lymphoblastoid cell line derived from blood leukocytes infected with EBV, B95-8 cells, as well as in EBV-positive Burkitt's lymphoma P3HR-1 cells (4). We examined an extended range of EBV-positive blood leukocyte cell lines as well as nasopharyngeal carcinoma cells, each of which was found to contain significant levels of BILF1-specific RNA.

Additionally, we showed that BILF1 transcription is dramatically upregulated upon phorbol ester treatment of latently infected cells, which induces EBV reactivation (49). This notion suggests that the EBV GPCR plays a role during productive infection rather than during latency.

In previous studies, the KSHV ORF74 gene has been implicated in the pathogenesis of Kaposi's sarcoma (3, 20, 23, 38). Similarly, the EBV GPCR may play a crucial role in the pathogenesis of EBV-induced diseases. It is therefore imperative to investigate the relationship between EBV GPCR-mediated signaling, as described in this report, and EBV infection in a wider perspective. As the BILF1-like genes are conserved among the genomes of all known gamma-1-herpesviruses, we expect this relation to be substantial.

ACKNOWLEDGMENTS

P.S.B. is supported by VENI grant 863.03.002 from the Netherlands Organization for Scientific Research (NWO). D.V. is supported by an NWO Jonge Chemici grant. M.J.S. and C.V. are supported by grants from the Royal Netherlands Academy of Arts and Sciences (KNAW).

We thank Servi Stevens and Jaap Middeldorp for generously supplying cell lines and RNA samples and Frank Stassen for critically reading the manuscript.

REFERENCES

1. **Arvanitakis, L., E. Geras-Raaka, A. Varma, M. C. Gershengorn, and E. Cesarman.** 1997. Human herpesvirus KSHV encodes a constitutively active G-protein-coupled receptor linked to cell proliferation. Nature **385:**347–350.
2. **Baer, R. J., A. T. Bankier, M. D. Biggin, P. L. Deininger, P. J. Farrell, T. J. Gibson, G. F. Hatfull, G. S. Hudson, S. C. Satchwell, C. Seguin, P. S. Tuffnell, and B. G. Barrell.** 1984. DNA sequence and expression of the B95-8 Epstein-Barr virus genome. Nature **310:**207–211.
3. **Bais, C., B. Santomasso, O. Coso, L. Arvanitakis, E. Geras-Raaka, J. S. Gutkind, A. S. Asch, E. Cesarman, M. C. Gershengorn, E. A. Mesri, and M. C. Gershengorn.** 1998. G-protein-coupled receptor of Kaposi's sarcoma-associated herpesvirus is a viral oncogene and angiogenesis activator. Nature **391:**86–89.
4. **Becker, Y., E. Tabor, and Y. Asher.** 1988. Leukemia. **2:**178S–191S.
5. **Beisser, P. S., C. Vink, J. G. van Dam, G. Grauls, S. J. Vanherle, and C. A. Bruggeman.** 1998. The R33 G protein-coupled receptor gene of rat cytomegalovirus plays an essential role in the pathogenesis of viral infection. J. Virol. **72:**2352–2363.
6. **Bodaghi, B., T. R. Jones, D. Zipeto, C. Vita, L. Sun, L. Laurent, F. Arenzana-Seisdedos, J.-L. Virelizier, and S. Michelson.** 1998. Chemokine sequestration by viral chemoreceptors as a novel viral escape strategy: withdrawal of chemokines from the environment of cytomegalovirus-infected cells. J. Exp. Med. **188:**855–866.
7. **Casarosa, P., R. A. Bakker, D. Verzijl, M. Navis, H. Timmerman, R. Leurs, and M. J. Smit.** 2001. Constitutive signaling of the human cytomegalovirus-encoded chemokine receptor US28. J. Biol. Chem. **276:**1133–1137.
8. **Casarosa, P., Y. K. Gruijthuijsen, D. Michel, P. S. Beisser, J. Holl, C. P. Fitzsimons, D. Verzijl, C. A. Bruggeman, T. Mertens, R. Leurs, C. Vink, and M. J. Smit.** 2003. Constitutive signaling of the human cytomegalovirus-encoded receptor UL33 differs from that of its rat cytomegalovirus homolog R33 by promiscuous activation of G proteins of the Gq, Gi, and Gs classes. J. Biol. Chem. **278:**50010–50023.
9. **Cole, K. E., C. A. Strick, T. J. Paradis, K. T. Ogborne, M. Loetscher, R. P. Gladue, W. Lin, J. G. Boyd, B. Moser, D. E. Wood, B. G. Sahagan, and K. Neote.** 1998. Interferon-inducible T cell alpha chemoattractant (I-TAC): a novel non-ELR CXC chemokine with potent activity on activated T cells through selective high affinity binding to CXCR3. J. Exp. Med. **187:**2009–2021.
10. **Couty, J. P., E. Geras-Raaka, B. B. Weksler, and M. C. Gershengorn.** 2001. Kaposi's sarcoma-associated herpesvirus G protein-coupled receptor signals through multiple pathways in endothelial cells. J. Biol. Chem. **276:**33805–33811.
11. **Davis-Poynter, N. J., and H. E. Farrell.** 1996. Masters of deception: a review of herpesvirus immune evasion strategies. Immunol. Cell. Biol. **74:**513–522.
12. **Davis-Poynter, N. J., D, M, Lynch, H. Vally, G. R. Shellam, W. D. Rawlinson, B. G. Barrell, and H. E. Farrell.** 1997. Identification and characterization of a G protein-coupled receptor homolog encoded by murine cytomegalovirus. J. Virol. **71:**1521–1529.
13. **Fluhmann, B., U. Zimmermann, R. Muff, G. Bilbe, J. A. Fisher, and W. Born.** 1998. Parathyroid hormone responses of cyclic AMP-, serum- and phorbol ester-responsive reporter genes in osteoblast-like UMR-106 cells. Mol. Cell. Endocrinol. **139:**159–161.
14. **Gao, J. L., and P. M. Murphy.** 1994. Hum. cytomegalovirus open reading frame US28 encodes a functional beta chemokine receptor. J. Biol. Chem. **269:**28539–288542.
15. **Geras-Raaka, E., A. Varma, H. Ho, I. Clark-Lewis, and M. C. Gershengorn.** 1998. Hum. interferon-gamma-inducible protein 10 (IP-10) inhibits constitutive signaling of Kaposi's sarcoma-associated herpesvirus G protein-coupled receptor. J. Exp. Med. **188:**405–408.
16. **Geras-Raaka, E., A. Varma, I. Clark-Lewis, I., and M. C. Gershengorn.** 1998. Kaposi's sarcoma-associated herpesvirus (KSHV) chemokine vMIP-II and human SDF-1alpha inhibit signaling by KSHV G protein-coupled receptor. Biochem. Biophys. Res. Commun. **253:**725–727.
17. **Gershengorn, M. C., E. Geras-Raaka, A. Varma, and I. Clark-Lewis.** 1998. Chemokines activate Kaposi's sarcoma-associated herpesvirus G protein-coupled receptor in mammalian cells in culture. J. Clin. Investig. **102:**1469–1472.
18. **Goldman, L. A., E. C. Cutrone, S. V. Kotenko, C. D. Krause, and J. A. Langer.** 1996. Modifications of vectors pEF-BOS, pcDNA1 and pcDNA3 result in improved convenience and expression. BioTechniques **21:**1013–1015.
19. **Gruijthuijsen, Y., K., P. Casarosa, S. J. Kaptein, J. L. Broers, R. Leurs, C. A. Bruggeman, M. J. Smit, and C. Vink.** 2002. The rat cytomegalovirus R33-encoded G protein-coupled receptor signals in a constitutive fashion. J. Virol. **76:**1328–1338.
20. **Guo, H. G., M. Sadowska, W. Reid, E. Tschachler, G. Hayward, and M. Reitz.** 2003. Kaposi's sarcoma-like tumors in a human herpesvirus 8 ORF74 transgenic mouse. J. Virol. **77:**2631–2639.
21. **Haskell, C. A., M. D. Cleary, and I. F. Charo.** 2000. Unique role of the chemokine domain of fractalkine in cell capture. Kinetics of receptor dissociation correlate with cell adhesion. J. Biol. Chem. **275:**34183–34189.
22. **Heston, L., M. Rabson, N. Brown, and G. Miller.** 1982. New Epstein-Barr virus variants from cellular subclones of P3J-HR-1 Burkitt lymphoma. Nature **295:**160–163.
23. **Holst, P. J., M. M. Rosenkilde, D. Manfra, S. C. Chen, M. T. Wiekowski, B. Holst, F. Cifire, M. Lipp, T. W. Schwartz, and S. A. Lira.** 2001. Tumorigenesis induced by the HHV8-encoded chemokine receptor requires ligand modulation of high constitutive activity. J. Clin. Investig. **108:**1789–1796.
24. **Hui, A. B., T. Cheung,.Y. Fong, K. W. Lo, and D. P. Huang.** 1998. Characterization of a new EBV-associated nasopharyngeal carcinoma cell line. Cancer Genet. Cytogenet. **101:**83–88.
25. **Kaptein, S. J., P. S. Beisser, Y. K. Gruijthuijsen, K. G. Savelkouls, K. W. van Cleef, E. Beuken, G. E. Grauls, C. A. Bruggeman, and C. Vink.** 2003. The rat cytomegalovirus R78 G protein-coupled receptor gene is required for production of infectious virus in the spleen. J. Gen. Virol. **84:**2517–2530.
26. **Kaufman, R. J.** 1999. Stress signaling from the lumen of the endoplasmic reticulum: coordination of gene transcriptional and translational controls. Genes Dev. **13:**1211–1233.
27. **Kilger, E., A. Kieser, M. Baumann, and M. Hammerschmidt.** 1998. Epstein-Barr virus-mediated B-cell proliferation is dependent upon latent membrane protein 1, which simulates an activated CD40 receptor. EMBO J. **17:**1700–1709.
28. **Kledal, T. N., M. M. Rosenkilde, and T. W. Schwartz.** 1998. Selective recognition of the membrane-bound CX3C chemokine, fractalkine, by the human cytomegalovirus-encoded broad-spectrum receptor US28. FEBS Lett. **441:**209–214.
29. **Klein, G., J. Zeuthen, P. Terasaki, R. Billing, R. Honig, M. Jondal, A. Westman, and G. Clements.** 1976. Inducibility of the Epstein-Barr virus (EBV) cycle and surface marker properties of EBV-negative lymphoma lines and their in vitro EBV-converted sublines. Int. J. Cancer **18:**639–652.
30. **Kozak, M.** 1987. An analysis of 5′-noncoding sequences from 699 vertebrate messenger RNAs. Nucleic Acids Res. **15:**8125–8148.
31. **Laemmli, U. K.** 1970. Cleavage of structural proteins during the assembly of the head of bacteriophage T4. Nature **227:**680–685.
32. **Lawrence, J. B., C. A. Villnave, and R. H. Singer.** 1988. Sensitive, high-resolution chromatin and chromosome mapping in situ: presence and orientation of two closely integrated copies of EBV in a lymphoma line. Cell **52:**51–61.
33. **Loetscher, M. L., B. Gerber, P. Loetscher, S. A. Jones, L. Piali, I. Clark-Lewis, M. Baggiolini, and B. Moser.** 1996. Chemokine receptor specific for IP10 and mig: structure, function, and expression in activated T-lymphocytes. J. Exp. Med. **184:**963–969.
34. **Meurs, E., K. Chong, J. Galabru, N. S. Thomas, I. M. Kerr, B. R. Williams, and A. G. Hovanessian.** 1990. Molecular cloning and characterization of the human double-stranded RNA-activated protein kinase induced by interferon. Cell **62:**379–390.
35. **Middeldorp, J. M., and P. Herbrink.** 1988. Epstein-Barr virus specific marker molecules for early diagnosis of infectious mononucleosis. J. Virol. Methods. **21:**133–146.
36. **Miller, G., and M. Lipman.** 1973. Release of infectious Epstein-Barr virus by transformed marmoset leukocytes. Proc. Natl. Acad. Sci. USA **70:**190–194.

37. **Miller, G., M. Rabson, and L. Heston.** 1984. Epstein-Barr virus with heterogeneous DNA disrupts latency. J. Virol. **50:**174–182.
38. **Montaner, S., A. Sodhi, A. Molinolo, T. H. Bugge, E. T. Sawai, Y. He, Y. Li, P. E. Ray, Pand J. S. Gutkind.** 2003. Endothelial infection with KSHV genes in vivo reveals that vGPCR initiates Kaposi's sarcomagenesis and can promote the tumorigenic potential of viral latent genes. Cancer Cell **3:**23–36.
39. **Murphy, P. M.** 2001. Viral exploitation and subversion of the immune system through chemokine mimicry. Nat. Immunol. **2:**116–122.
40. **Oliveira, S. A., and T. E. Shenk.** 2001. Murine cytomegalovirus M78 protein, a G protein-coupled receptor homologue, is a constituent of the virion and facilitates accumulation of immediate-early viral mRNA. Proc. Natl. Acad. Sci. USA **98:**3237–3242.
41. **Oudejans, J. J., M. Jiwa, A. J. van den Brule, F. A. Grasser, A. Horstman, W. Vos, P. M. Kluin, P. van der Valk, J. M. Walboomers, and C. J. Meijer.** 1995. Detection of heterogeneous Epstein-Barr virus gene expression patterns within individual post-transplantation lymphoproliferative disorders. Am. J. Pathol. **147:**923–933.
42. **Ploegh, H. L., L. E. Cannon, and L. J. Strominger.** 1979. Cell-free translation of the mRNAs for the heavy and light chains of HLA-A and HLA-B antigens. Proc. Natl. Acad. Sci. USA **76:**2273–2277.
43. **Poppers, J., M. Mulvey, C. Perez, D. Khoo, and I. Mohr.** 2003. Identification of a lytic-cycle Epstein-Barr virus gene product that can regulate PKR activation. J. Virol. **77:**228–236.
44. **Rickinson, A. B., and E. Kieff.** 2001. Epstein-Barr virus, p. 2575–2627. *In* D. M. Knipe and P. M. Howley (ed.), Fields virology, 4th ed. Lippincott & Wilkins, Philadelphia, Pa.
45. **Shepard, L. W., M. Yang, P. Xie, D. D. Browning, T. Voyno-Yasenetskaya, T. Kozasa, and R. D. Ye.** 2001. Constitutive activation of NF-kappa B and secretion of interleukin-8 induced by the G protein-coupled receptor of Kaposi's sarcoma-associated herpesvirus involve G alpha(13) and RhoA. J. Biol. Chem. **276:**45979–45987.
46. **Smit, M. J., D. Verzijl, P. Casarosa, M. Navis, H. Timmerman, and R. Leurs.** 2002. Kaposi's sarcoma-associated herpesvirus-encoded G protein-coupled receptor ORF74 constitutively activates p44/p42 MAPK and Akt via G_i and phospholipase C-dependent signaling pathways. J. Virol. **76:**1744–1752.
47. **Smit, M. J., C. Vink, D. Verzijl, P. Casarosa, C. A. Bruggeman, and R. Leurs.** 2003. Virally encoded G protein-coupled receptors: targets for potentially innovative anti-viral drug development. Curr. Drug. Targets **4:**431–441.
48. **Streblow, D. N., C. Soderberg-Naucler, J. Vieira, P. Smith, E. Wakabayashi, F. Ruchti, K. Mattison, Y. Altschuler, and J. A. Nelson.** 1999. The human cytomegalovirus chemokine receptor US28 mediates vascular smooth muscle cell migration. Cell **99:**511–520.
49. **Van Grunsven, W. M., A. Nabbe, and J. M. Middeldorp.** 1993. Identification and molecular characterization of two diagnostically relevant marker proteins of the Epstein-Barr virus capsid antigen complex. J. Med. Virol. **40:**161–169.
50. **Vuyisich, M., R. J. Spanggord, and P. A. Beal.** 2002. The binding site of the RNA-dependent protein kinase (PKR) on EBER1 RNA from Epstein-Barr virus. EMBO Rep. **3:**622–627.
51. **Waldhoer, M., T. N. Kledal, H. Farrell, and T. W. Schwartz.** 2002. Murine cytomegalovirus (CMV) M33 and human CMV US28 receptors exhibit similar constitutive signaling activities. J. Virol. **76:**8161–8168.
52. **Williams, B. R. G.** 1999. PKR; a sentinel kinase for cellular stress. Oncogene **18:**6112–6120.
53. **Wu, D., A. Katz, and M. I. Simon.** 1993. Activation of phospholipase C β_2 by the α and $\beta\gamma$ subunits of trimeric GTP-binding protein. Proc. Natl. Acad. Sci. USA **90:**5297–5301.